nature biotechnology

Nutrient-sensitized screening for drugs that shift energy metabolism from mitochondrial respiration to glycolysis

Vishal M Gohil[1–3,7], Sunil A Sheth[1–3,7], Roland Nilsson[1–3], Andrew P Wojtovich[4,5], Jeong Hyun Lee[6], Fabiana Perocchi[1–3], William Chen[1–3], Clary B Clish[2], Cenk Ayata[6], Paul S Brookes[4,5] & Vamsi K Mootha[1–3]

Most cells have the inherent capacity to shift their reliance on glycolysis relative to oxidative metabolism, and studies in model systems have shown that targeting such shifts may be useful in treating or preventing a variety of diseases ranging from cancer to ischemic injury. However, we currently have a limited number of mechanistically distinct classes of drugs that alter the relative activities of these two pathways. We screen for such compounds by scoring the ability of >3,500 small molecules to selectively impair growth and viability of human fibroblasts in media containing either galactose or glucose as the sole sugar source. We identify several clinically used drugs never linked to energy metabolism, including the antiemetic meclizine, which attenuates mitochondrial respiration through a mechanism distinct from that of canonical inhibitors. We further show that meclizine pretreatment confers cardioprotection and neuroprotection against ischemia-reperfusion injury in murine models. Nutrient-sensitized screening may provide a useful framework for understanding gene function and drug action within the context of energy metabolism.

Virtually all cells exhibit metabolic flexibility and are capable of shifting their reliance on glycolysis relative to mitochondrial respiration. Such shifts can occur at different timescales through a variety of mechanisms, allowing cells to cope with prevailing nutrient availability or energetic demands. There is mounting evidence of the therapeutic potential of targeting such shifts. For example, many cancer cells rely on aerobic glycolysis (the Warburg effect)[1], and a recent study has shown that pharmacological agents that shift their metabolism toward mitochondrial respiration can retard tumor growth[2]. Conversely, studies in animal models have shown that attenuating mitochondrial respiration can prevent the pathological consequences of ischemia-reperfusion injury in myocardial infarction and stroke[3–7].

These observations motivate the search for agents that can safely induce shifts in cellular energy metabolism in humans. Promising work in this area has focused on hypoxia-inducible factor (HIF)[8], a well-studied transcriptional regulator of genes involved in the cellular adaptation to hypoxia[9,10]. HIF inhibitors and activators have been identified through both academic and pharmaceutical drug screens and exhibit preclinical efficacy in treating cancer[11] and in ischemic disease[12], respectively. Other approaches to treat ischemic injury include induced hypothermia, which has met with mixed results[13]. New classes of agents, that can be titrated to safely shift energy metabolism, may yet provide important therapeutic value in several human diseases.

Here we use a nutrient-sensitized screening strategy to identify drugs that shift cellular energy metabolism based on their selective effect on cell growth and viability in glucose- versus galactose-containing media. Nutrient-sensitized screening is based on the evidence that mammalian cells redirect their energy metabolism in response to the available sugar source[14]. Culturing cells in galactose as the sole sugar source forces mammalian cells to rely on mitochondrial oxidative phosphorylation (OXPHOS) and was previously used to diagnose human mitochondrial disorders or drug toxicity[15,16]. By screening our chemical library for drugs that selectively inhibit cell growth and proliferation in galactose- relative to glucose-containing media, we identify several FDA-approved compounds that redirect oxidative metabolism to glycolysis. We pursue the mechanism and potential clinical utility of one drug, meclizine, which is available without prescription, crosses the blood-brain barrier and has never, to our knowledge, been linked to energy metabolism.

RESULTS

A metabolic state–dependent growth and viability assay

Consistent with previous studies focused on other cell types[14,17], we found that human MCH58 skin fibroblasts grown in glucose derive ATP from both aerobic glycolysis and mitochondrial glutamine oxidation (**Fig. 1**). However, when these cells are grown in galactose they exhibit a five- to sixfold decrease in the extracellular acidification rate (ECAR)[18], reflecting decreased glycolysis, and a twofold increase in the oxygen consumption rate (OCR), consistent with a switch to glutamine oxidation[14] (**Fig. 1b**,**c**). Moreover, cells grown in galactose-containing medium maximize mitochondrial ATP production by using a larger fraction of mitochondrial respiration for ATP synthesis (**Supplementary Fig. 1**).

[1]Center for Human Genetic Research, Massachusetts General Hospital, Boston, Massachusetts, USA. [2]Broad Institute of Massachusetts Institute of Technology and Harvard, Cambridge, Massachusetts, USA. [3]Department of Systems Biology, Harvard Medical School, Boston, Massachusetts, USA. [4]Department of Pharmacology and Physiology and [5]Department of Anesthesiology, University of Rochester Medical Center, Rochester, New York, USA. [6]Stroke and Neurovascular Regulation Laboratory, Department of Radiology, Massachusetts General Hospital, Charlestown, Massachusetts, USA. [7]These authors contributed equally to this work. Correspondence should be addressed to V.K.M. (vamsi@hms.harvard.edu).

Received 23 November 2009; accepted 12 January 2010; published online 14 February 2010; doi:10.1038/nbt.1606

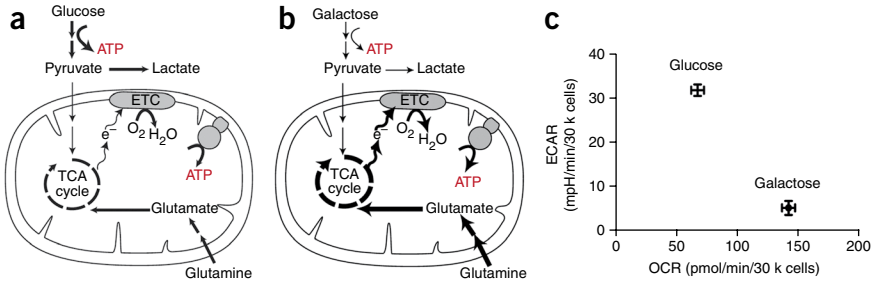

Figure 1 Metabolic plasticity of human fibroblasts. (**a**,**b**) Schematic representation of cellular energy metabolism pathways. (**a**) Cells grown in glucose-rich medium derive ATP from glycolysis as well as from glutamine-driven respiration. TCA, tricarboxylic acid; ETC, electron transport chain. (**b**) Replacing glucose with galactose forces cells to generate ATP almost exclusively from glutamine-driven oxidative metabolism[14]. (**c**) Measurement of ECAR, a proxy for the rate of glycolysis, and OCR, a proxy for mitochondrial respiration, of fibroblasts grown in media containing 10 mM glucose or 10 mM galactose for 3 d. Data are expressed as mean ± s.d. ($n = 5$).

The metabolic flexibility of fibroblasts permits screening for compounds that retard growth or are lethal to cells only in a given metabolic state. In a pilot experiment, we confirmed nutrient-dependent drug sensitivity of fibroblasts to known inhibitors of OXPHOS (**Supplementary Fig. 2**). To screen a library of chemicals, we designed a high-throughput microscopy-based growth assay to identify compounds that differentially affect growth and viability in galactose- relative to glucose-containing media (**Fig. 2a** and **Supplementary Fig. 3a**). Because the proliferation rates are higher for cells provided with glucose instead of galactose as their sole sugar source (**Supplementary Fig. 3b**), we considered the normalized cell number in each of the two nutrient conditions. By measuring growth and survival over a 3-day period, we were able to increase our ability to discover compounds with even subtle effects on energy metabolism.

A small-molecule screen for agents that shift energy metabolism

We screened a library of 3,695 chemical compounds in duplicate. The library has been previously described[19] and consists of two commercially available compound collections that span nearly half of all FDA-approved drugs, as well as other bioactives and natural products. We analyzed the glucose and galactose results jointly to assign each drug a score, $S_{glu/gal}$, defined as the log ratio of the normalized cell number in glucose divided by the normalized cell number in galactose. The full table of results is provided in **Supplementary Table 1**.

Positive $S_{glu/gal}$ scores indicate drugs that were selectively lethal or inhibited growth in galactose-containing medium, such as inhibitors of OXPHOS. Negative $S_{glu/gal}$ scores may arise from inhibition of glycolysis or from inhibition of proliferation, as fibroblasts cultured in glucose grow more rapidly (**Supplementary Fig. 3b**). For most drugs, $S_{glu/gal}$ is close to zero, indicating similar effects on growth and viability in glucose- and galactose-containing media (**Fig. 2b** and **Supplementary Table 1**). Reassuringly, the upper tail of the $S_{glu/gal}$ distribution (**Fig. 2b**) is highly enriched for known respiratory chain and OXPHOS inhibitors: the top 25 compounds include 20 compounds previously known to disrupt respiration by directly interrupting mitochondrial respiration or uncoupling it from ATP synthesis (**Supplementary Table 2**). Conversely, the lower tail is enriched for known antineoplastic agents (**Fig. 2b**): 14 of the 25 lowest $S_{glu/gal}$ scores correspond to known chemotherapeutic agents that are likely to retard the growth and viability of cells rapidly proliferating in glucose (**Supplementary Table 3**).

We next asked if any clinically used drugs exhibit high $S_{glu/gal}$ scores. Among the top 2% of the $S_{glu/gal}$ distribution (83 compounds), we identified 25 agents that have been used clinically (**Supplementary Table 4**). Previous reports provide evidence that 9 out of these 25 drugs (papaverine, phenformin, artemisinin, pentamidine (NebuPent), clomiphene (Clomid), pimozide (Orap), niclosamide, fluvastatin (Lescol), carvedilol (Coreg)) can directly inhibit or uncouple the mitochondrial respiratory chain (**Supplementary Table 4**). This list includes two antimalarial drugs (mefloquine (Lariam) and artemisinin), the latter of which has been reported to require mitochondrial respiration in the malarial parasite for its action[20]. The remaining 16 clinically used agents cover a broad range of indications and diverse mechanisms of action and, to our knowledge, have never been linked to energy metabolism. We were particularly interested in identifying compounds that induce subtle metabolic shifts, as they may represent particularly safe drugs with which to manipulate energy metabolism. To this end, we focused on commercially available drugs exhibiting low to intermediate, positive $S_{glu/gal}$ scores (0.15–0.45). We carried out secondary assays of OCR, ECAR and cell viability and confirmed

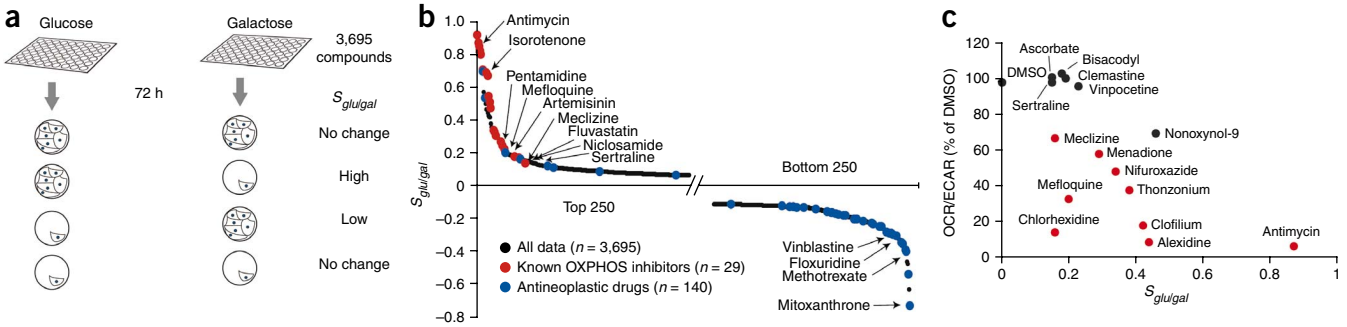

Figure 2 A nutrient-sensitized screen to discover agents that shift energy metabolism. (**a**) Schematic of the drug screen. MCH58 fibroblasts grown in 96-well plates in glucose- or galactose-containing media are exposed to a chemical library of 3,695 compounds for 72 h. The logarithm of the normalized cell number in glucose versus galactose provides a summary statistic ($S_{glu/gal}$) for each compound. (**b**) Results from a nutrient-sensitized screen. $S_{glu/gal}$ is plotted for top and bottom 250 compounds. (**c**) Secondary assays to evaluate compounds with modest yet positive $S_{glu/gal}$ scores. The OCR/ECAR ratio of selected compounds is plotted against the compounds' corresponding $S_{glu/gal}$ score from **b**. OCR and ECAR measurements were made on MCH58 fibroblasts grown in glucose and are normalized to cell viability. Compounds indicated by red symbols exhibited a statistically significant decrease in the OCR/ECAR ratio based on at least three independent replicates ($P < 0.05$; two-sided t-test).

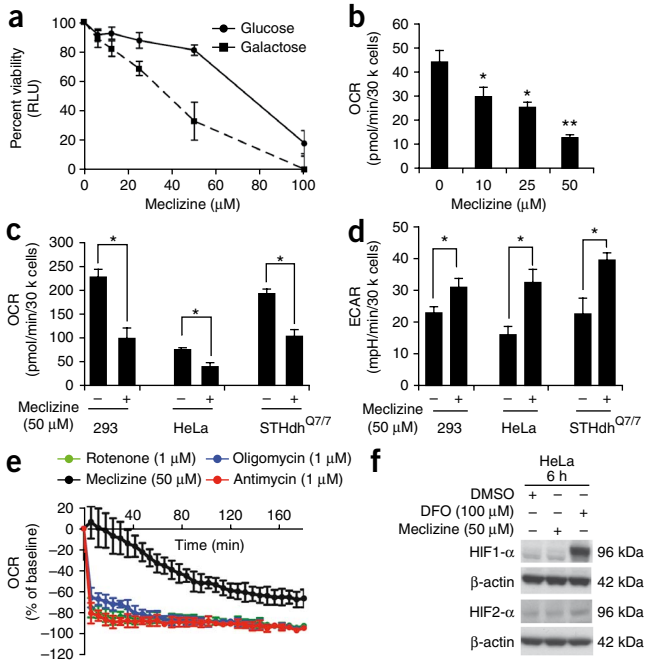

Figure 3 Effects of meclizine on cellular energy metabolism. (**a**) Cell viability of MCH58 fibroblasts cultured in glucose- or galactose-containing media with varying doses of meclizine for 3 d. Data are expressed as mean ± s.d. ($n = 5$). (**b**) OCR in MCH58 fibroblasts cultured in glucose-containing medium with varying doses of meclizine for 200 min. Data are expressed as mean ± s.d. ($n = 3$). (*, $P < 0.05$; **, $P < 0.005$; two-sided *t*-test). (**c**,**d**) OCR (**c**) and ECAR (**d**) in multiple cell types cultured in glucose-containing medium with 50 μM meclizine or DMSO for 200 min. Data are expressed as mean ± s.d. ($n \geq 3$). (*, $P < 0.05$; two-sided *t*-test). (**e**) Time course of meclizine (50 μM)-mediated OCR reduction over DMSO baseline compared to other inhibitors of OXPHOS (1 μM each) in HEK293 cells. Data are expressed as mean ± s.d. ($n \geq 3$). (**f**) HIF-1α and HIF-2α detection by western blot analysis of protein extract from HeLa cells after 6-h treatment with 0.1% DMSO, 100 μM deferoxamine (DFO) or 50 μM meclizine. The complete immunoblot is provided as **Supplementary Figure 7b**.

that eight of these agents induce statistically significant ($P < 0.05$) metabolic shifts (**Fig. 2c**). Of these eight clinically used drugs, we were particularly interested in meclizine (Antivert), which has been approved for the treatment of nausea and vertigo for decades, is available over the counter, has a favorable safety profile, and likely penetrates the blood-brain barrier given its efficacy in disorders of the central nervous system[21].

Meclizine attenuates respiration in intact cells

In secondary assays, we replicated our screening result and confirmed that galactose-grown cells are more sensitive to increasing doses of meclizine (**Fig. 3**). In agreement with our secondary screening assay (**Fig. 2c**), treatment with meclizine reduced the OCR in a dose-dependent manner in cells cultured in glucose-rich medium (**Fig. 3b**). Meclizine-induced reduction in OCR and concomitant increase in ECAR occurred in all cell types tested, including immortalized mouse striatal cells, human embryonic kidney cells (HEK293) and HeLa cells (**Fig. 3c–d** and **Supplementary Fig. 4**). Although meclizine is classified as a histamine receptor (H_1) antagonist and a weak muscarinic acetylcholine receptor antagonist[22], the other 64 annotated H_1 receptor antagonists and 33 annotated antimuscarinic antagonists in our chemical library did not exhibit elevated $S_{glu/gal}$ scores (anticholinergic $P = 0.26$, anti-H_1 $P = 0.77$; Mann-Whitney rank sum test). We tested two classic antihistamines—pyrilamine and pheniramine as well as two well-characterized antimuscarinic agents—atropine and scopolamine for their ability to inhibit OCR. Unlike meclizine, these agents did not inhibit cellular OCR (**Supplementary Fig. 5**). These results suggest that meclizine's effect on energy metabolism occurs by means of a mechanism not involving cholinergic or histamine receptors.

Meclizine's suppression of cellular oxygen consumption occurred with much slower kinetics than canonical inhibitors of OXPHOS that directly target the respiratory chain or ATP synthase (**Fig. 3e**). The slow kinetics suggest that it takes time for meclizine to accumulate in mitochondria or alternatively, that it might act indirectly. To distinguish between these alternatives, we studied the effect of meclizine on isolated mitochondria. Using glutamate and malate, pyruvate and malate or succinate as fuel substrates, we found no effect of meclizine on respiration of isolated mitochondria (**Fig. 4a–c**). Meclizine did not have

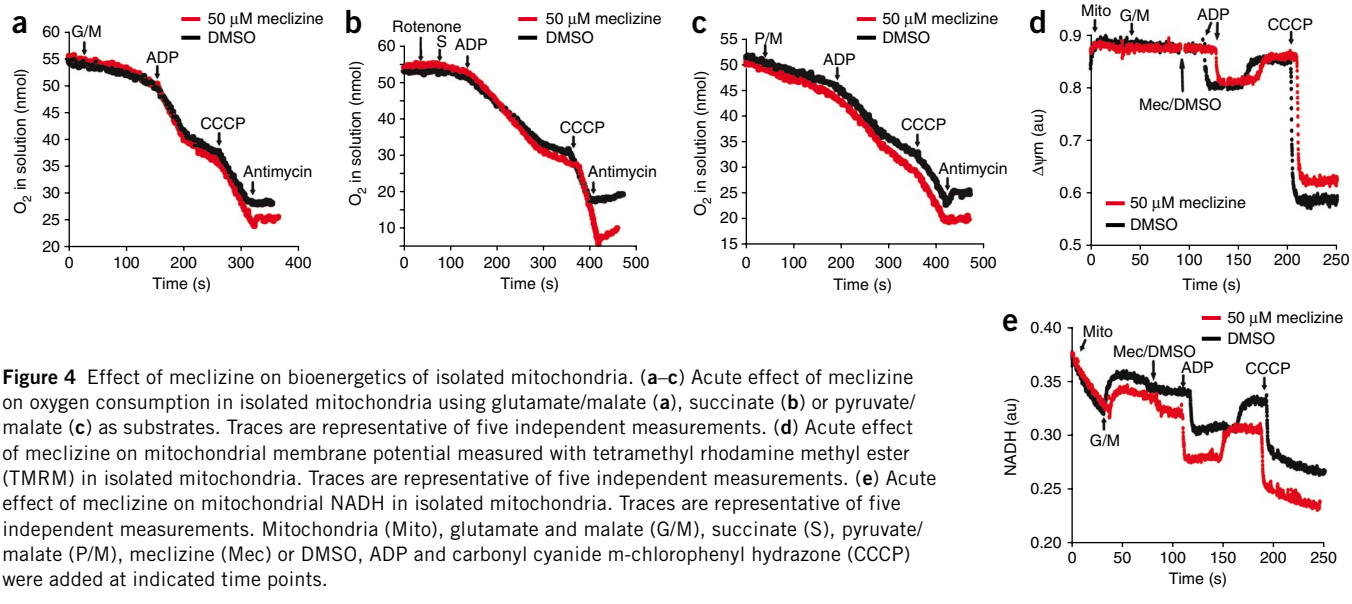

Figure 4 Effect of meclizine on bioenergetics of isolated mitochondria. (**a**–**c**) Acute effect of meclizine on oxygen consumption in isolated mitochondria using glutamate/malate (**a**), succinate (**b**) or pyruvate/malate (**c**) as substrates. Traces are representative of five independent measurements. (**d**) Acute effect of meclizine on mitochondrial membrane potential measured with tetramethyl rhodamine methyl ester (TMRM) in isolated mitochondria. Traces are representative of five independent measurements. (**e**) Acute effect of meclizine on mitochondrial NADH in isolated mitochondria. Traces are representative of five independent measurements. Mitochondria (Mito), glutamate and malate (G/M), succinate (S), pyruvate/malate (P/M), meclizine (Mec) or DMSO, ADP and carbonyl cyanide m-chlorophenyl hydrazone (CCCP) were added at indicated time points.

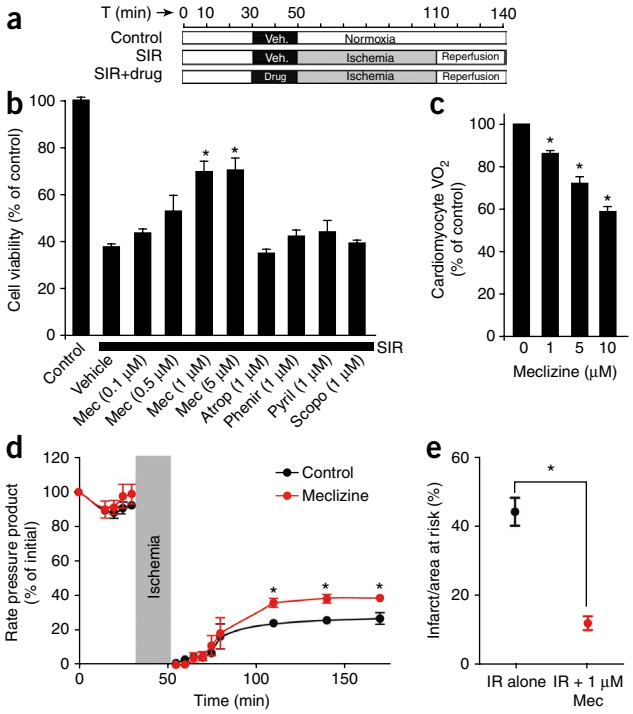

Figure 5 Meclizine is cardioprotective in cellular and *ex vivo* models of cardiac ischemia. (**a**) Protocol for the simulated ischemia-reperfusion (SIR) injury model. (**b**) Viability of adult rat cardiomyocytes subjected to SIR injury, in the presence of indicated concentrations of meclizine (Mec), atropine (Atrop), pheniramine (Phenir), pyrilamine (Pyril) and scopolamine (Scopo). (**c**) Respiration of cardiomyocytes after exposure to indicated concentrations of meclizine. (**d**,**e**) Langendorff perfused rat hearts were subjected to 25 min of global ischemia followed by 2 h of reperfusion. Meclizine treatment comprised infusion of 1 μM meclizine from a port above the aortic cannula for 20 min, followed by a 1-min wash-out before ischemia. (**d**) Rate pressure product (heart rate × left ventricular developed pressure) is expressed as a percentage of the initial value throughout the ischemia-reperfusion (IR) protocol. (**e**) Following IR, hearts were stained with TTC and infarct size was quantified. All data are means ± s.e.m. from four to six individual experiments. (*, $P < 0.05$, ANOVA in **d**, Student's *t*-test in **e**).

a qualitative impact on membrane potential or redox potential during respiratory state transitions of isolated mitochondria (**Fig. 4d**,**e**). Furthermore, meclizine treatment had no effect on mitochondrial morphology, membrane potential, mitochondrial (mt) DNA copy number or the expression of mtRNAs in intact cells (**Supplementary Fig. 6**). Collectively, these observations demonstrate that unlike classic inhibitors or uncouplers such as rotenone, antimycin, oligomycin or carbonyl cyanide m-chlorophenyl hydrazone, meclizine does not itself directly inhibit and/or uncouple the OXPHOS machinery in isolated mitochondria, and does not reduce mitochondrial biogenesis in intact cells. Instead it may act through novel signaling or transcriptional mechanisms.

Activation of HIF1-α or HIF2-α is known to induce transcriptional rewiring of energy metabolism from mitochondrial respiration to glycolysis[23]. However, unlike with deferoxamine, a known inducer of the HIF pathway, we did not observe HIF1-α or HIF2-α stabilization after meclizine treatment (**Fig. 3f** and **Supplementary Fig. 7a**,**b**). Moreover, the kinetics of meclizine's OCR inhibition argue against a transcriptional mechanism, as meclizine treatment resulted in inhibition within 2 h, whereas OCR inhibition mediated by deferoxamine only became apparent after 12 h (**Supplementary Fig. 7c**). In addition, we examined the effect of meclizine treatment on HIF-responsive genes using an HIF response element-luciferase reporter construct and recorded no induction of luciferase activity after a 6-h treatment (**Supplementary Fig. 7d**).

Collectively, these studies suggest that meclizine inhibits mitochondrial respiration indirectly, in an HIF-independent manner that does not involve histaminergic or muscarinic receptor signaling.

Meclizine pretreatment confers protection against ischemic injury

Previous studies have clearly established that brief, nonlethal episodes of ischemia can confer prophylaxis against subsequent stroke or myocardial infarction, and studies in model systems have shown that chemical inhibition of mitochondrial respiration can mimic this protection, a process coined "chemical preconditioning"[6]. Having shown that meclizine, an over-the-counter drug that crosses the blood-brain barrier can attenuate mitochondrial respiration, we sought to determine whether this drug is cardioprotective and neuroprotective in cellular and animal models.

First, we tested meclizine in an adult rat ventricular cardiomyocyte model of simulated ischemia-reperfusion injury (**Fig. 5a**). A 20-min meclizine pre-incubation followed by wash-out before ischemia elicited a dose-dependent protection of cardiomyocytes against cell death, whereas other antihistamines (pyrilamine and pheniramine) and antimuscarinic agents (scopolamine and atropine) did not provide protection (**Fig. 5b**). These results are consistent with the hypothesis that mild OXPHOS inhibition is cytoprotective in ischemic injury. As with the other cell types, meclizine inhibited oxygen consumption in cardiomyocytes in a dose-dependent manner (**Fig. 5c** and **Supplementary Fig. 8a**,**b**) but not in isolated cardiac mitochondria (**Supplementary Fig. 8c**,**d**). Next, we tested whether meclizine protects isolated, perfused rat hearts from ischemia-reperfusion injury in an *ex vivo* model of ischemic injury. Meclizine preserved heart pump function after the ischemic event (**Fig. 5d**) and significantly ($P < 0.05$) reduced the infarct area of Langendorff perfused rat hearts subjected to 25 min of global ischemia (**Fig. 5e**).

Chemical preconditioning has also been shown to be protective in animal models of cerebral ischemia[6,12,24–26]. To determine whether meclizine might similarly be useful in this context, we first established safety and pharmacokinetic parameters for an intraperitoneal dosing regimen (see Online Methods). We found that mice tolerate daily intraperitoneal injections of 100 mg/kg meclizine without any weight loss or behavioral changes even after four consecutive days. Six hours after a single intraperitoneal dose, the plasma concentration is in the 3–5 μM range, a concentration sufficient to attenuate mitochondrial respiration of primary mouse neurons (**Supplementary Fig. 9**). We then tested whether meclizine protects against cerebral ischemia by pretreating mice with two intraperitoneal injections of 100 mg/kg meclizine, or an equal volume of vehicle at 17 h and 3 h before a 1 h transient middle cerebral artery occlusion (**Fig. 6**). We found that total infarct volume was significantly reduced by 23% in meclizine-treated animals ($P = 0.03$, **Fig. 6c**). In addition, meclizine significantly reduced the area of infarction in brain slices with the greatest area of infarct ($P = 0.02$, **Fig. 6d**,**e**). The *in vivo* protective effect of meclizine is likely independent of its antihistamine or antimuscarinic property, as treatment with pyrilamine or scopolamine did not decrease infarct volume (**Fig. 6c**) or reduce the area of infarction in brain slices (**Fig. 6d**,**e**). Furthermore, meclizine-pretreated animals tended toward having preserved neurological function compared to controls ($P = 0.07$, Kruskal-Wallis non-parametric ANOVA).

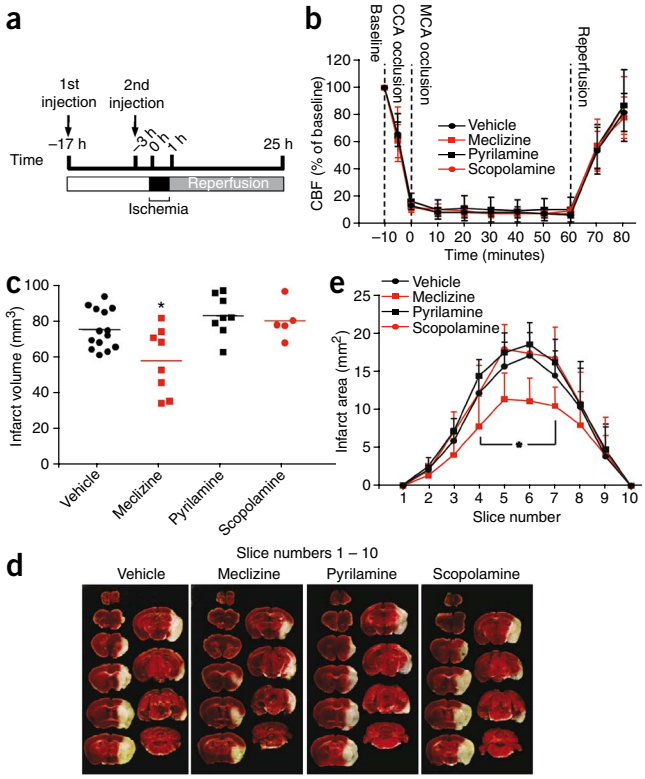

Figure 6 Meclizine is neuroprotective in a mouse model of stroke. (**a**) Protocol for the murine model of stroke. Male C57BL/6 mice were treated with two intraperitoneal injections of 100 mg/kg meclizine, 20 mg/kg pyrilamine and 0.5 mg/kg scopolamine or vehicle at 17 h and 3 h before 1 h transient middle cerebral artery occlusion followed by 24 h of reperfusion. (**b**) Cerebral blood flow (CBF) measured at baseline and after occlusion of the common carotid artery (CCA) and middle cerebral artery (MCA) upon treatment with meclizine, scopolamine, pyrilamine or vehicle. Data represent mean ± s.d. (**c**) Infarct volume measured on TTC-stained 1-mm thick coronal slices obtained from mice treated with meclizine, scopolamine, pyrilamine or vehicle. Data points refer to independent experiments, and the solid line represents their mean. (*$P < 0.05$ versus vehicle and scopolamine, $P < 0.01$ versus pyrilamine; one-way ANOVA followed by Tukey's multiple comparison test). (**d**) Representative images of TTC-stained 1-mm thick coronal brain sections (slice 1–10). (**e**) Infarct area in the rostrocaudal extent of the brain (slice 1–10) upon treatment with meclizine, scopolamine, pyrilamine or vehicle. Data points represent the mean area of infarction in individual slice levels ± s.d. in mm^2 ($n = 14$ for vehicle, $n = 8$ for meclizine, $n = 8$ for pyrilamine, $n = 5$ for scopolamine, *$P < 0.05$).

The cerebral blood flow deficit (**Fig. 6b**) and the amount of post-operative weight loss did not differ between the groups.

DISCUSSION

Recent studies have shown that changes in cellular energy metabolism can accompany a range of human diseases, and that targeting energy metabolism may hold therapeutic potential. However, we lack an arsenal of clinically safe and useful agents that target energy metabolism by distinct mechanisms. In this study, we have introduced a facile, nutrient-sensitized screening strategy aimed at identifying small molecules that shift cellular energy metabolism from mitochondrial respiration to glycolysis. We have identified several FDA-approved drugs that exhibit such activity and may have potential for helping to abrogate ischemia-reperfusion injury in the heart, brain and perhaps other sensitive organ systems such as the lung or kidney. Focusing on one specific hit from our screen, meclizine, we have demonstrated that it suppresses OXPHOS by means of a mechanism distinct from classic inhibitors or uncouplers, and that it confers protection against cardiac and cerebral ischemia in cellular and animal models.

A large body of literature demonstrates that agents that blunt mitochondrial respiration can offer prophylaxis against cell death after ischemia and reperfusion in the heart[4,5,27] or brain[3,6,26]. This effect is thought to occur through suppressing oxidative injury, and may be related to protection conferred by ischemic preconditioning, although the precise molecular mechanism is not known. Notably, redirecting energy metabolism toward glycolysis can reduce oxidative damage and suppresses apoptosis[28–30]. Interestingly, switching to anaerobic metabolism appears to be a natural adaptation to reduced oxygen availability[31], and activation of the HIF pathway provides one such strategy for redirecting energy metabolism toward glycolysis[9,32]. Recent studies using genetic and chemical approaches of activating the HIF pathway have shown promising results in various models of ischemia-reperfusion injury. For example, myofibers of prolyl hydroxylase 1 knockout mice are resistant to acute ischemia because of reduced generation of oxidative stress[33]. In preclinical studies, prolyl hydroxylase inhibitors confer protection in models of myocardial infarction[34], stroke[35] and renal ischemia[36]. However, as HIF regulates the expression of a plethora of genes, and unwanted side effects have remained a concern[37], it might be useful to expand the arsenal of agents that shift energy metabolism.

Our screen has identified a new metabolic activity for meclizine, an over-the-counter drug that has been in use in the United States for >40 years for treatment of nausea and vertigo. We found that 1 μM meclizine pretreatment provided cytoprotection in *in vitro* and *ex vivo* models of cardiac ischemia-reperfusion injury (**Fig. 5**). In addition, we showed that prophylaxis with meclizine significantly reduced infarct volume in an *in vivo* model of cerebral ischemia (**Fig. 6**). The utility of pretreatment paradigms described in this study arises in clinical settings in which ischemic insults can be anticipated. Examples of such situations include patients undergoing high-risk surgical procedures and the large cohort of patients that suffer from diseases of recurrent ischemia, such as unstable angina or recurrent transient ischemic attacks[38]. An open question is whether currently approved doses of meclizine achieve the required blood concentrations required for cardioprotection or neuroprotection. Post-marketing surveillance data support the safe nonprescription use of meclizine, and published studies in animals, including nonhuman primates, have shown that higher doses can be tolerated[39,40]. However, because the potency of meclizine in attenuating mitochondrial respiration appears to vary across cell types (**Figs. 3c** and **5c** and **Supplementary Fig. 9**), preclinical studies of efficacy and toxicity are required to rigorously determine optimal dosing and safety regimens before evaluating the utility of meclizine for new clinical indications in humans.

Our detailed studies on the effects of meclizine on cellular energy metabolism clearly show that it attenuates mitochondrial respiration in a manner distinct from other drugs of known mechanism of action and independent of the HIF pathway (**Fig. 3f** and **Supplementary Fig. 7**). In contrast to canonical inhibitors, meclizine does not directly target the OXPHOS machinery in isolated mitochondria (**Fig. 4**) and can be titrated over a broad range of concentrations to achieve inhibition of cellular OCR by 10–60% (**Fig. 3b**). Our data suggest that meclizine acts independently of the muscarinic or histamine receptors, as drugs affecting these two receptors did not inhibit OCR (**Supplementary Fig. 5**) and they do not confer neuroprotection or cytoprotection in our models (**Figs. 5** and **6**). We do not know the precise molecular target

of meclizine responsible for this effect on energy metabolism, but one possibility is a metabolic target outside the mitochondrion whose subsequent impact is to direct metabolism away from OXPHOS. Alternatively, meclizine may undergo a bio-transformation into a product that directly inhibits the OXPHOS machinery. We cannot exclude the possibility that meclizine, like many clinically used drugs, hits multiple cellular targets to affect cellular energetics and confer cytoprotection.

Nutrient-sensitized screening, as we have presented it, builds on previous studies that have shown that many cultured cells generate their ATP from either glycolysis or glutamine oxidation[14,17]. However, the screening strategy may not necessarily work in other cell types, for example, cells with limited metabolic flexibility, cells that do not have pathways for glutamine oxidation, or postmitotic cells in which a growth assay is not possible. Another limitation of our approach is that the compounds that emerge from the screen may act not only on energy-related pathways, but also potentially on other properties influenced by the switch in nutrients. For example, we have noted that cells grown in glucose tend to proliferate more quickly, and for this reason, drugs from the right side of the tail (**Fig. 2b**) could either be blunting glycolytic metabolism or affecting rapid proliferation. Hence, secondary assays are still required to confirm the energetic consequences of a drug identified by our screening assay.

Our screen contained only a few thousand compounds and has already shown high sensitivity for identifying drugs that target cellular pathways of energy metabolism. As we have shown here, compounds emerging from the upper tail of the distribution (**Fig. 2b** and **Supplementary Tables 2** and **4**) could serve as valuable lead compounds for prophylaxis against heart attack and stroke, but they may also find broader application for preventing or treating a wide variety of other diseases involving oxidative damage, such as neurodegenerative disorders. The opposite tail includes dozens of compounds already used as chemotherapeutic agents, perhaps due to their selective toxicity in more rapidly proliferating cells, and may include additional, clinically safe agents that could be useful as adjuvant therapies. The results of our screen may help to pinpoint clinical benefits (or toxicity) of drugs that are not readily attributable to their known targets or mechanism of action. We anticipate that this strategy can be extended to other nutrients—such as fatty acids or ketone bodies. The nutrient-sensitized assay can also be used to screen a much larger library of compounds or even genome-wide RNA interference perturbations to systematically understand drug action and gene function within the broader context of cellular energy homeostasis.

METHODS

Methods and any associated references are available in the online version of the paper at http://www.nature.com/naturebiotechnology/.

Availability of raw data. Screening data in the form of cell count per well are available at ChemBank for galactose plates (http://chembank.broadinstitute.org/assays/view-assay.htm?xn=1020.0120) and glucose plates (http://chembank.broadinstitute.org/assays/view-assay.htm?xn=1020.0121).

Note: Supplementary information is available on the Nature Biotechnology website.

ACKNOWLEDGMENTS

We thank E. Shoubridge for the MCH58 cell line; M. MacDonald for immortalized striatal cells; R. Xavier for the HRE luciferase construct; S. Norton, B. Wagner and the Broad Chemical Screening Platform for assistance in compound arraying; J. Evans of the Whitehead Institute/MIT BioImaging Center for assistance with high-throughput microscopy; C. Belcher-Timme for technical assistance; T. Kitami for assistance with mitochondrial imaging; M. Mehta for assistance reviewing drug toxicity data; S. Calvo, A. Chess, R. Gould, E. Lander, A. Ting, S. Vafai and members of Mootha lab for valuable discussions and comments. This work was supported by fellowships or grants from the United Mitochondrial Disease Foundation (V.M.G.); Howard Hughes Medical Institute (S.A.S. and V.K.M.); National Institutes of Health (RO1 HL-071158 to P.S.B.); Deane Institute for Integrative Research in Stroke and Atrial Fibrillation (C.A.); American Heart Association (#0815770D to A.P.W.); the Burroughs Wellcome Fund (V.K.M.); the Center for Integration of Medical and Innovative Technology (V.K.M.); and the American Diabetes Association/Smith Family Foundation (V.K.M.).

AUTHOR CONTRIBUTIONS

V.M.G. and V.K.M. conceived the project; V.M.G., S.A.S., J.H.L., W.C., F.P., C.B.C. and A.P.W. performed experiments; V.M.G., S.A.S., J.H.L., R.N., F.P., C.A., P.S.B. and V.K.M. performed statistical and data analysis; V.M.G., S.A.S. and V.K.M. wrote the paper.

COMPETING INTERESTS STATEMENT

The authors declare competing financial interests: details accompany the full-text HTML version of the paper at http://www.nature.com/naturebiotechnology/.

Published online at http://www.nature.com/naturebiotechnology/.
Reprints and permissions information is available online at http://npg.nature.com/reprintsandpermissions/.

1. Warburg, O. On the origin of cancer cells. *Science* **123**, 309–314 (1956).
2. Bonnet, S. *et al.* A mitochondria-K+ channel axis is suppressed in cancer and its normalization promotes apoptosis and inhibits cancer growth. *Cancer Cell* **11**, 37–51 (2007).
3. Huber, R., Spiegel, T., Buchner, M. & Riepe, M.W. Graded reoxygenation with chemical inhibition of oxidative phosphorylation improves posthypoxic recovery in murine hippocampal slices. *J. Neurosci. Res.* **75**, 441–449 (2004).
4. Burwell, L.S., Nadtochiy, S.M. & Brookes, P.S. Cardioprotection by metabolic shut-down and gradual wake-up. *J. Mol. Cell. Cardiol.* **46**, 804–810 (2009).
5. Chen, Q., Camara, A.K., Stowe, D.F., Hoppel, C.L. & Lesnefsky, E.J. Modulation of electron transport protects cardiac mitochondria and decreases myocardial injury during ischemia and reperfusion. *Am. J. Physiol. Cell Physiol.* **292**, C137–C147 (2007).
6. Riepe, M.W. *et al.* Increased hypoxic tolerance by chemical inhibition of oxidative phosphorylation: "chemical preconditioning". *J. Cereb. Blood Flow Metab.* **17**, 257–264 (1997).
7. Piantadosi, C.A. & Zhang, J. Mitochondrial generation of reactive oxygen species after brain ischemia in the rat. *Stroke* **27**, 327–331 (1996).
8. Kaelin, W.G. Jr. & Ratcliffe, P.J. Oxygen sensing by metazoans: the central role of the HIF hydroxylase pathway. *Mol. Cell* **30**, 393–402 (2008).
9. Kim, J.W., Tchernyshyov, I., Semenza, G.L. & Dang, C.V. HIF-1-mediated expression of pyruvate dehydrogenase kinase: a metabolic switch required for cellular adaptation to hypoxia. *Cell Metab.* **3**, 177–185 (2006).
10. Fukuda, R. *et al.* HIF-1 regulates cytochrome oxidase subunits to optimize efficiency of respiration in hypoxic cells. *Cell* **129**, 111–122 (2007).
11. Semenza, G.L. Defining the role of hypoxia-inducible factor 1 in cancer biology and therapeutics. *Oncogene* published online, doi:10.1038/onc.2009.441 (30 November 2009).
12. Fraisl, P., Aragones, J. & Carmeliet, P. Inhibition of oxygen sensors as a therapeutic strategy for ischaemic and inflammatory disease. *Nat. Rev. Drug Discov.* **8**, 139–152 (2009).
13. Hoesch, R.E. & Geocadin, R.G. Therapeutic hypothermia for global and focal ischemic brain injury–a cool way to improve neurologic outcomes. *Neurologist* **13**, 331–342 (2007).
14. Reitzer, L.J., Wice, B.M. & Kennell, D. Evidence that glutamine, not sugar, is the major energy source for cultured HeLa cells. *J. Biol. Chem.* **254**, 2669–2676 (1979).
15. Robinson, B.H., Petrova-Benedict, R., Buncic, J.R. & Wallace, D.C. Nonviability of cells with oxidative defects in galactose medium: a screening test for affected patient fibroblasts. *Biochem. Med. Metab. Biol.* **48**, 122–126 (1992).
16. Marroquin, L.D., Hynes, J., Dykens, J.A., Jamieson, J.D. & Will, Y. Circumventing the Crabtree effect: replacing media glucose with galactose increases susceptibility of HepG2 cells to mitochondrial toxicants. *Toxicol. Sci.* **97**, 539–547 (2007).
17. DeBerardinis, R.J. *et al.* Beyond aerobic glycolysis: transformed cells can engage in glutamine metabolism that exceeds the requirement for protein and nucleotide synthesis. *Proc. Natl. Acad. Sci. USA* **104**, 19345–19350 (2007).
18. Wu, M. *et al.* Multiparameter metabolic analysis reveals a close link between attenuated mitochondrial bioenergetic function and enhanced glycolysis dependency in human tumor cells. *Am. J. Physiol. Cell Physiol.* **292**, C125–C136 (2007).
19. Wagner, B.K. *et al.* Large-scale chemical dissection of mitochondrial function. *Nat. Biotechnol.* **26**, 343–351 (2008).
20. Golenser, J., Waknine, J.H., Krugliak, M., Hunt, N.H. & Grau, G.E. Current perspectives on the mechanism of action of artemisinins. *Int. J. Parasitol.* **36**, 1427–1441 (2006).
21. The Food and Drug Administration Antiemetic drug products for over-the-counter human use; final monograph. *Fed. Regist.* **52**, 15866–15893 (1987).

22. Brunton, L.L., Lazo, J.S. & Parker, K.L.. *Goodman & Gilman's The Pharmacological Basis of Therapeutics*, edn. 11 (The McGraw-Hill Companies, 2006).
23. Papandreou, I., Cairns, R.A., Fontana, L., Lim, A.L. & Denko, N.C. HIF-1 mediates adaptation to hypoxia by actively downregulating mitochondrial oxygen consumption. *Cell Metab.* **3**, 187–197 (2006).
24. Gidday, J.M. Cerebral preconditioning and ischaemic tolerance. *Nat. Rev. Neurosci.* **7**, 437–448 (2006).
25. Sugino, T., Nozaki, K., Takagi, Y. & Hashimoto, N. 3-Nitropropionic acid induces ischemic tolerance in gerbil hippocampus *in vivo*. *Neurosci. Lett.* **259**, 9–12 (1999).
26. Ratan, R.R. *et al.* Translation of ischemic preconditioning to the patient: prolyl hydroxylase inhibition and hypoxia inducible factor-1 as novel targets for stroke therapy. *Stroke* **35**, 2687–2689 (2004).
27. Lesnefsky, E.J. *et al.* Blockade of electron transport during ischemia protects cardiac mitochondria. *J. Biol. Chem.* **279**, 47961–47967 (2004).
28. Jeong, D.W., Kim, T.S., Cho, I.T. & Kim, I.Y. Modification of glycolysis affects cell sensitivity to apoptosis induced by oxidative stress and mediated by mitochondria. *Biochem. Biophys. Res. Commun.* **313**, 984–991 (2004).
29. Hunter, A.J., Hendrikse, A.S. & Renan, M.J. Can radiation-induced apoptosis be modulated by inhibitors of energy metabolism? *Int. J. Radiat. Biol.* **83**, 105–114 (2007).
30. Vaughn, A.E. & Deshmukh, M. Glucose metabolism inhibits apoptosis in neurons and cancer cells by redox inactivation of cytochrome c. *Nat. Cell Biol.* **10**, 1477–1483 (2008).
31. Ramirez, J.M., Folkow, L.P. & Blix, A.S. Hypoxia tolerance in mammals and birds: from the wilderness to the clinic. *Annu. Rev. Physiol.* **69**, 113–143 (2007).
32. Lu, C.W., Lin, S.C., Chen, K.F., Lai, Y.Y. & Tsai, S.J. Induction of pyruvate dehydrogenase kinase-3 by hypoxia-inducible factor-1 promotes metabolic switch and drug resistance. *J. Biol. Chem.* **283**, 28106–28114 (2008).
33. Aragones, J. *et al.* Deficiency or inhibition of oxygen sensor Phd1 induces hypoxia tolerance by reprogramming basal metabolism. *Nat. Genet.* **40**, 170–180 (2008).
34. Philipp, S. *et al.* Stabilization of hypoxia inducible factor rather than modulation of collagen metabolism improves cardiac function after acute myocardial infarction in rats. *Eur. J. Heart Fail.* **8**, 347–354 (2006).
35. Siddiq, A. *et al.* Hypoxia-inducible factor prolyl 4-hydroxylase inhibition. A target for neuroprotection in the central nervous system. *J. Biol. Chem.* **280**, 41732–41743 (2005).
36. Bernhardt, W.M. *et al.* Preconditional activation of hypoxia-inducible factors ameliorates ischemic acute renal failure. *J. Am. Soc. Nephrol.* **17**, 1970–1978 (2006).
37. Brahimi-Horn, M.C. & Pouyssegur, J. Harnessing the hypoxia-inducible factor in cancer and ischemic disease. *Biochem. Pharmacol.* **73**, 450–457 (2007).
38. Dirnagl, U., Becker, K. & Meisel, A. Preconditioning and tolerance against cerebral ischaemia: from experimental strategies to clinical use. *Lancet Neurol.* **8**, 398–412 (2009).
39. Giurgea, M. & Puigdevall, J. Experimental teratology with Meclozine. *Med. Pharmacol.* **15**, 375–388 (1966).
40. Lione, A. & Scialli, A.R. The developmental toxicity of the H1 histamine antagonists. *Reprod. Toxicol.* **10**, 247–255 (1996).

ONLINE METHODS

All experiments were done in accordance with the national and institutional guidelines for animal welfare, adhering to protocols approved by the institutional subcommittee on research animal care.

Cell culture. Immortalized MCH58 human diploid fibroblasts containing the pLKO.1 vector were grown in DMEM high-glucose medium (Invitrogen) with 10% FBS (Sigma), 1× penicillin, streptomycin and glutamine (Invitrogen), 2 μl/ml puromycin and 50 μg/ml uridine at 37 °C and 5% CO_2. The high-glucose medium was replaced with 10 mM glucose or 10 mM galactose wherever indicated. All media contained 1 mM pyruvate and 4 mM glutamine. MCH58 fibroblasts (without pLKO.1), HeLa and HEK293 cells were grown in DMEM high-glucose medium with 10% FBS at 37 °C and 5% CO_2; STHdh$^{Q7/7}$ mouse striatal cells were grown at 33 °C.

Measurement of cellular OCR and ECAR. OCR and ECAR measurements were carried out as previously described[18] with minor modifications. Briefly, MCH58 fibroblasts were seeded in XF24-well cell culture microplates (Seahorse Bioscience) at 30,000 cells/well in 10 mM glucose- or 10 mM galactose–containing media and incubated at 37 °C and 5% CO_2 for ~20 h. Before the measurements were made, the growth medium was replaced with ~925 μl of assay medium (with 10 mM glucose or 10 mM galactose as the sugar source) and cells were incubated at 37 °C for 60 min. The OCR and ECAR measurements on HeLa, HEK293 and STHdh$^{Q7/7}$ mouse striatal cells were carried out by growing them in XF24 plates at 40,000/well (HeLa and STHdh$^{Q7/7}$ mouse striatal cells) or 50,000/well (HEK293 cells) for ~20 h under their regular growth conditions, as described in the previous section. The assay medium was the same as above except 25 mM glucose was used as the sugar source. Three baseline measurements were recorded before the addition of compounds. For the secondary screening assay on selected compounds listed in **Figure 2c**, MCH58 fibroblasts were grown in 25 mM glucose-containing medium in the presence of a compound for 16–20 h. Each compound was tested at screening concentration—antimycin (3.65 μM), ascorbate (10 μM), clofilium tosylate (5.9 μM), nifuroxazide (7.27 μM), meclizine (10 μM), menadione (11.62 μM), clemastine (5.82 μM), vinpocetine (5.71 μM), bisacodyl (5.53 μM), nonoxynol-9 (10 μM), sertraline (10 μM), thonzonium (3.91 μM), chlorhexidine (3.96 μM), mefloquine (10 μM) and alexidine (3.93 μM). OCR measurements on the mouse primary cortical neurons obtained from day E14–15 embryos were carried out in their regular growth medium.

Cell viability assays. MCH58 fibroblasts were seeded in 96-well plates at 5,000 cells/well in DMEM high-glucose medium. After ~20 h, cells were washed in PBS and the growth medium was replaced with 10 mM glucose- or 10 mM galactose-containing media containing different concentrations of meclizine, rotenone, antimycin, oligomycin or DMSO (0.1%). The cells were then grown for 72 h and cell viability was assayed by the CellTiter-Glo Luminescent Viability assay (Promega).

Chemical screening and high-throughput assay of cell number quantification. MCH58 fibroblasts were seeded at 5,000 cells/well using the robotic MultiDrop Combi (ThermoFisher Scientific) dispenser into 96-well plates (PerkinElmer) at 100 μl per well in DMEM high-glucose medium. Twenty-four hours later, cells were washed twice in PBS and medium was replaced with either 10 mM glucose- or 10 mM galactose-containing media. Approximately 100 nl of each compound was pin-transferred in duplicate into the plates with a steel pin array using the CyBi-Well robot (CyBio). The compound collection of 3,695 drugs includes two commercially available libraries (Spectrum and Prestwick). Compound-treated plates were incubated at 37 °C for 72 h. Cells were then washed once with PBS, stained with 10 μM Hoechst 33342 (Invitrogen) and fixed in 3.7% formaldehyde solution for 15 min. Wells were then washed once and stored in PBS. Cell culture plates were stored at 4 °C until the time of imaging, which was at most 24 h after fixation. Imaging was performed by Arrayscan VTi automated microscope (ThermoFisher Scientific) with the use of an automated plate stacker at the Whitehead Institute Biomedical Imaging Center. Four nonoverlapping images at 5× magnification (NA 0.25) were acquired for a field of view of 1.3 mm × 1.3 mm per image. Image analysis was performed using the freely available open-source software package CellProfiler[41]. Images were analyzed individually by first identifying nuclei using the Hoechst staining signal. Total number of nuclei per field were recorded, and the sum of nuclei from four images per well gave cell count per well. Computation was performed using a UNIX computer cluster. The unprocessed data from our screen in the form of cell count per well are available in ChemBank. Please note that the ChemBank data sets include statistical calculations that were not used in our final analysis. For a detailed description of our statistical methods, please refer to the section below "Statistical analysis of screening data," which outlines the method used to calculate our summary statistic, $S_{glu/gal}$. The $S_{glu/gal}$ value for every compound included in our screen can be found in **Supplementary Table 1**.

Assays of mitochondrial physiology. Mitochondria were isolated from C57BL/6 mouse kidneys by differential centrifugation and resuspended in experimental buffer as described previously[42], to a final concentration of 0.5 mg/ml. State 2 respiration was initiated with the addition of 12.5 mM glutamate and 12.5 mM malate, or 20 mM pyruvate and 1 mM malate or 12 mM succinate and 3 μM rotenone. State 3 respiration was initiated with the addition of 0.2 mM ADP, and uncoupled respiration was initiated with the addition of 5 μM carbonyl cyanide m-chlorophenyl hydrazone. Mitochondria were incubated for 5 min in respiration buffer pH 7.4 supplemented with either meclizine (50 μM) or DMSO. O_2 consumption was monitored with a Fiber Optic Oxygen sensor probe (Ocean Optics) at 25 °C, and NADH (endogenous, 370 ± 7 nm excitation, 440 ± 4 nm emission) and membrane potential (1.25 μM TMRM, 546 ± 7 nm excitation, 590 ± 4 nm emission) were measured with a Perkin-Elmer LS50B luminescence spectrometer.

Drug testing in cardiac ischemia-reperfusion injury. Adult rat ventricular cardiomyocytes were isolated by endotoxin-free collagenase perfusion, and the simulated ischemia-reperfusion injury was performed as previously described[43]. Briefly, ischemia comprised 1 h in anoxic glucose-free buffer at pH 6.5, and reperfusion comprised 30 min in normoxic glucose-replete buffer at pH 7.4. Cell viability was monitored by Trypan blue exclusion. Rat cardiac mitochondria were isolated, and respiration of both cells and mitochondria was measured using a Clark oxygen electrode, as previously described[44]. Isolated rat hearts were retrograde reperfused in Langendorff mode under constant flow as described previously[45].

Drug testing in neuronal ischemia-reperfusion injury. Plasma concentrations of meclizine were determined after intraperitoneal injections in C57BL/6 mice. Injections of 100 mg/kg meclizine or vehicle control were followed by cardiac puncture blood draws at 1 h or 6 h. Absolute concentrations of meclizine in plasma were measured using liquid chromatography tandem mass spectrometry against a purified standard. To check the protective effect of the tested compounds, male C57BL/6 mice were treated with two intraperitoneal injections of 100 mg/kg meclizine, 20 mg/kg pyrilamine and 0.5 mg/kg scopolamine or vehicle, 17 h and 3 h before ischemia. Drug doses for pyrilamine and scopolamine were chosen based on previous literature evidence of *in vivo* brain bioavailability[46,47]. The experimenter was blinded to treatment groups. Mice were anesthetized with isoflurane (2.5% induction, 1.5% maintenance, in 70% N_2O/30% O_2), and subjected to 1 h transient middle cerebral artery occlusion using an intraluminal filament inserted through the external carotid artery. Regional cerebral blood flow was monitored using a laser Doppler probe placed over the core middle cerebral artery territory. Rectal temperature was controlled at 37 °C by a servo-controlled heating pad. Total infarct volume was calculated on 2,3,5-triphenyltetrazolium chloride (TTC)-stained 1-mm thick coronal sections by integrating the infarct areas in each of ten slice levels. Infarct volume was calculated using the 'indirect method', that is, contralateral hemisphere minus ipsilateral non-infarcted volume. Data were expressed as mean ± s.d. One-way ANOVA followed by Tukey's multiple comparison test was used for analysis of values between groups. Neurological deficit scores were analyzed by Kruskal-Wallis nonparametric ANOVA followed by Dunn's multiple comparisons test. $P < 0.05$ was considered statistically significant.

Western blot analysis. HIF1-α and HIF2-α stabilization was assessed in MCH58 fibroblasts and HeLa cells by carrying out western blot detection using anti-HIF1-α (Cell Signaling) and anti-HIF2-α (Novus Biologicals) antibodies.

doi:10.1038/nbt.1606

Protein was extracted from cells pretreated with either 0.1% DMSO, 50 μM meclizine or 100 μM deferoxamine (Sigma). SDS PAGE was performed on 15 μg/lane protein using NuPAGE 4–12% Bis-Tris gel from Invitrogen. Western blot analysis was performed as per the standard procedures. β-actin was used as a loading control.

HIF reporter assay. Luciferase activity in HeLa cells transiently transfected with HIF response element (HRE)/luciferase construct was measured by the Dual-Luciferase Reporter Assay System (Promega). The drug treatment was initiated ~24 h after the transfection and the treatment was continued for 6 h with 0.1% DMSO, 100 μM deferoxamine or 50 μM meclizine. HeLa cells were transfected using the Fugene reagent (Roche) as per the manufacturer's instruction. HRE reporter construct was a generous gift from R. Xavier, Massachusetts General Hospital.

Assays of mitochondrial abundance, morphology and membrane potential in intact cells. Mitochondrial (mt) morphology, membrane potential, mtDNA content and mtDNA expression were measured in HeLa cells treated with 50 μM of meclizine over a 6-h period. MitoTracker CMXRos (Invitrogen) and Hoechst 33342 staining of live cells was performed as per manufacturer's recommendation. The stained cells were observed at 20× magnification with an Olympus CKX41 microscope and fluorescent images were captured with a QiCAM camera. The mitochondrial membrane potential was measured with a ratiometric dye, JC-1 by measuring relative fluorescent units at 590 nm and 535 nm using a fluorescent plate reader. The mtDNA copy number and mtRNA transcripts were measured by quantitative real-time PCR assays as described previously[48].

Drug annotation. All FDA-approved drugs were annotated after confirming their entry in the Orange book, 29th edition 2009. For other clinically used compounds, we used the corresponding PubMed and PubChem entries.

Statistical analysis of screening data. Normalized cell counts were computed separately for each 96-well plate by dividing the cell count of each well with the trimmed mean (the average after discarding the largest and smallest value) of the cell counts for the 16 DMSO-treated wells on each plate. A single 96-well plate exhibited very low counts in all wells and was discarded. We then removed measurements that failed to replicate by requiring that the ratio of normalized counts was <1.5 between replicates; this excluded 49 wells. The remaining replicate measurements were averaged, and fold changes were computed as the ratio between the averaged normalized counts for the glucose and galactose screens. The $S_{glu/gal}$ for each compound was calculated by taking the $\log_{10}$ of the normalized and averaged fold change in glucose divided by galactose. To evaluate statistical significance, we computed Z-scores for each well against the DMSO (null) distribution and averaged Z-scores across replicates. Wells with average Z-score > 2.5 were considered significant.

41. Carpenter, A.E. *et al.* CellProfiler: image analysis software for identifying and quantifying cell phenotypes. *Genome Biol.* **7**, R100 (2006).
42. Mootha, V.K., Arai, A.E. & Balaban, R.S. Maximum oxidative phosphorylation capacity of the mammalian heart. *Am. J. Physiol.* **272**, H769–H775 (1997).
43. Wojtovich, A.P. & Brookes, P.S. The complex II inhibitor atpenin A5 protects against cardiac ischemia-reperfusion injury via activation of mitochondrial KATP channels. *Basic Res. Cardiol.* **104**, 121–129 (2009).
44. Wojtovich, A.P. & Brookes, P.S. The endogenous mitochondrial complex II inhibitor malonate regulates mitochondrial ATP-sensitive potassium channels: implications for ischemic preconditioning. *Biochim. Biophys. Acta* **1777**, 882–889 (2008).
45. Nadtochiy, S.M., Tompkins, A.J. & Brookes, P.S. Different mechanisms of mitochondrial proton leak in ischaemia/reperfusion injury and preconditioning: implications for pathology and cardioprotection. *Biochem. J.* **395**, 611–618 (2006).
46. Miyazaki, S., Imaizumi, M. & Onodera, K. Effects of thioperamide, a histamine H3-receptor antagonist, on a scopolamine-induced learning deficit using an elevated plus-maze test in mice. *Life Sci.* **57**, 2137–2144 (1995).
47. Toyota, H. *et al.* Behavioral characterization of mice lacking histamine H(3) receptors. *Mol. Pharmacol.* **62**, 389–397 (2002).
48. Baughman, J.M. *et al.* A computational screen for regulators of oxidative phosphorylation implicates SLIRP in mitochondrial RNA homeostasis. *PLoS Genet.* **5**, e1000590 (2009).